Mitigation of Soil-Structure Interaction in Integral Bridge Abutments through Geogrid Reinforcement under Seasonal Thermal and Traffic Loading

Qiuhong Zhao (1), Kui Gui (2), Youqun Wang (3), Songlin Zhang (4), Baochun Chen (5), Zhihua Chen (6)

(1) *Professor, Tianjin Chengjian University, zhao@tcu.edu.cn*
(2) *PhD Candidate, Tianjin University, kg_kui@tju.edu.cn*
(3) *PhD Candidate, Tianjin University, youqunwang@tju.edu.cn*
(4) *Master Student, Tianjin University, 2023205221@tju.edu.cn*
(5) *Professor, Fujian University of Technology, baochunchen@fzu.edu.cn*
(6) *Professor, Tianjin University, zhchen@tju.edu.cn*

Abstract

In Integral Abutment Bridges (IABs), the thermally induced expansion and contraction of the superstructure (main girder and deck) drive the abutments into longitudinal reciprocating motion. This cyclic movement inevitably leads to significant distress, specifically the ratcheting effect (cumulative build-up) of lateral earth pressures as well as progressive deformation of the backfill. To effectively address these issues, this paper proposes the use of geogrid reinforcement to mitigate the Soil-Structure Interaction in integral bridge abutments, reducing both the lateral earth pressure ratcheting as well as the deformation of the backfill.

A 1g small-scale physical model was constructed for this study, in which the model abutment was subjected to 100 horizontal displacement cycles to simulate its service-life reciprocating motion. Concurrently, vertical cyclic loads were applied to the model approach slab to replicate the axle loads of design vehicles. Through two series of model tests, the lateral earth pressure ratcheting and backfill deformation induced by soil-structure interaction were evaluated. Experimental results demonstrate that geogrid reinforcement effectively suppresses the cyclic ratcheting of both passive earth pressure and backfill settlement, while significantly attenuating peak lateral pressure levels. Compared to the unreinforced group, the peak passive earth pressure coefficient and maximum cumulative settlement were reduced by approximately 50.2% and 50%, respectively.

Keywords: *Integral bridge; Soil structure interaction; Geogrid reinforcement; Passive lateral earth pressure; Settlement*

1. Introduction

Integral Abutment Bridges (IABs) offer distinct economic and durability advantages by eliminating expansion joints; however, the cyclic longitudinal displacements of the abutment, driven by the thermal expansion and contraction of the superstructure, induce complex soil-structure interaction (SSI). This long-term cyclic action not only triggers the ratcheting of passive earth pressure behind the abutment [1] but also leads to significant backfill settlement [2]. Such settlement causes the approach slab to lose its vertical bedding support at one end, thereby necessitating the redistribution of traffic loads toward the far end of the slab [3], which further compromises the long-term serviceability of the slab-soil system. Furthermore, studies indicate that the attributes of vertical vehicular loading, particularly frequency and magnitude, can exacerbate surface settlement[4]. Consequently, developing robust backfill treatment technologies to mitigate lateral pressure escalation and control settlement remains a critical engineering challenge for the widespread implementation of IABs.

To address these challenges, a series of 1g scaled physical model tests were performed to evaluate the engineering efficacy of geogrid reinforcement in suppressing lateral earth pressure ratcheting and mitigating backfill settlement under the coupled influence of seasonal thermal cycles and traffic loading. This work establishes a rigorous scientific basis for the optimized design of the integrated abutment-approach slab-soil system in IABs.

2. Testing program

2.1 Test setup

The experimental apparatus comprised a rigid model container equipped with independent horizontal and vertical loading systems. To ensure sufficient structural rigidity during testing, the container was fabricated from welded square hollow steel sections and steel plates. The horizontal loading system employed four servo-controlled screw jacks to precisely simulate the kinematic displacement modes of the abutment. Concurrently, a servo-controlled vertical loading system was utilized to replicate vehicular axle loads. Comprehensive technical specifications and geometric dimensions of the physical model are detailed in Wang et al. (2026).

Using the Cass County Bridge as a prototype, a physical model of the abutment system was constructed at a geometric scale of 1:5. The approach slab, sleeper slab, and pavement layer were scaled to a uniform thickness of 0.05 m, with the approach and sleeper slabs measuring 1.07 m and 0.3 m in length, respectively. The vertical traffic load was applied at a distance of 0.65 m from the abutment. The instrumentation layout is illustrated in Figure 1. The experimental program comprised two distinct test configurations: an unreinforced backfill (T1) and a geogrid-reinforced backfill (T2).

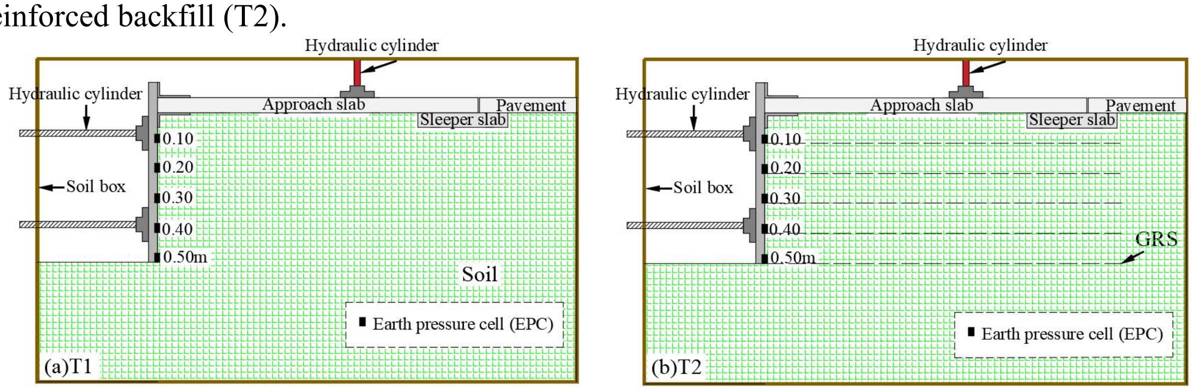

Fig. 1 Experimental configurations

2.2 Material

To ensure material consistency, sieved river sand was employed as the backfill. Preliminary characterization of its physical properties yielded a median particle size (D_{50}) of 0.2 mm, a coefficient of uniformity (C_u) of 1.74, a coefficient of curvature (C_c) of 1.0, and a peak internal friction angle of 40.9°. Comprehensive details regarding the backfill soil are available in Wang et al. (2026). In this study, the bridge abutment was idealized as a rigid body and fabricated from a 50-mm-thick and 600-mm-high steel plate. The approach slab, pavement layer, and sleeper slab were all cast using C30-grade concrete. Furthermore, the geogrid reinforcement was composed of high-density polyethylene.

2.3 Loading scheme

Building upon the research of Liu et al (2022) and Wang et al (2026), a coupled loading protocol was implemented in this study. Figures 2a and 2b illustrate the horizontal displacement history of the abutment and the vertical force profile, which were designed to emulate seasonal thermal variations and traffic loading, respectively. Specifically, each complete horizontal reciprocating cycle was partitioned into four distinct stages (①–④) to represent a full annual thermal cycle. To simulate a 100-year design life, a total of 100 horizontal cycles were applied. During the experimental procedure, at each of the four designated horizontal positions (I–IV), the abutment displacement was held constant while 100 vertical load cycles were applied to the approach slab. This coupled loading sequence was executed iteratively until the conclusion of the loading program.

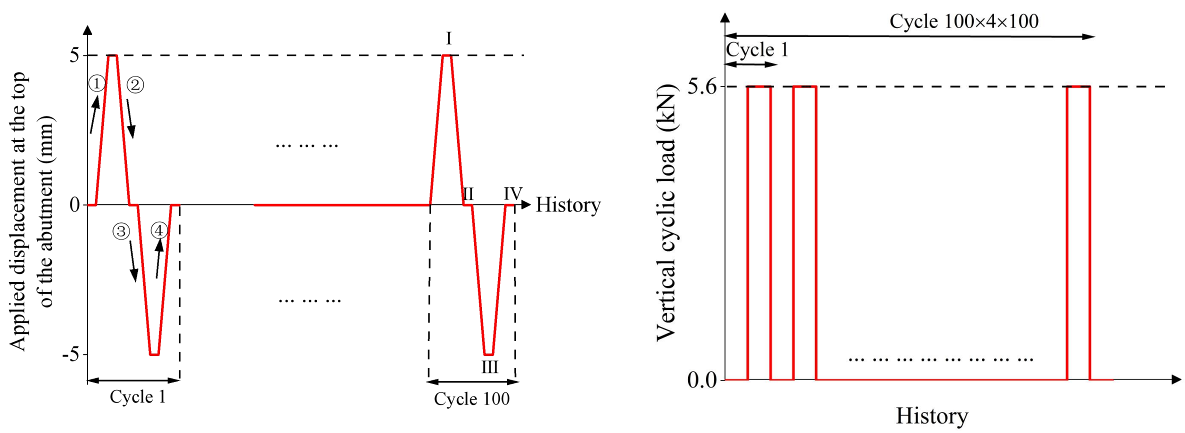

(a) Horizontal cyclic displacement at the abutment top (b) Vertical cyclic load on the approach slab

Fig. 2 Loading scheme

3. Analysis and discussion

3.1 Passive lateral earth pressure

Figure 3 illustrates the evolution of the passive lateral earth pressure for both the T1 and T2 groups. As depicted in Fig. 3(a), the passive earth pressure coefficient ($K_{m,p}$) for the T1 group exhibited a progressive build-up with the increasing number of cycles, culminating in a peak value of 23.1 at the 60th cycle. This response reflects pronounced cyclic ratcheting of the backfill. Subsequently, $K_{m,p}$ leveled off, entering a stable plateau phase. In contrast, Group T2 exhibited a markedly different evolution pattern for the passive earth pressure coefficient ($K_{m,p}$). During the initial three loading cycles, $K_{m,p}$ rose marginally from 7.8 to 10.2; however, from the fourth cycle onward, the coefficient remained constrained within a narrow band of 11 – 12, demonstrating remarkable stability. Compared to the T1 group, the peak $K_{m,p}$ in Group T2 was attenuated by approximately 50.2%. This suggests that the geogrid reinforcement effectively mitigates the cyclic accumulation of passive lateral earth pressure, enabling the backfill to reach a steady state shortly after the onset of loading.

Figure 3(b) illustrates the vertical distribution of passive lateral earth pressures along the abutment height after 100 cycles. For the T1 group, the pressure profile exhibited a characteristic bilinear distribution, reaching a peak magnitude of 154.9 kPa at a depth of approximately 0.4 m. This distinct distribution pattern highlights a pronounced stress concentration, reflecting the severe cyclic ratcheting effect developed within the unreinforced backfill. Conversely, the passive lateral earth pressures in the T2 reinforced configuration were markedly lower than those observed in the T1 group. At the corresponding elevation of -0.4 m, the peak passive pressure decreased sharply to approximately 57.5 kPa, representing a reduction of over 60%. Although the T2 group exhibited relatively high earth pressures near the abutment base (around an elevation of -0.5 m), the peak magnitude in the mid-to-lower section was substantially suppressed, yielding a more uniform and gradual distribution profile. These results demonstrate that the geogrid reinforcement significantly mitigates the peak lateral thrust and promotes a more homogeneous pressure distribution, thereby effectively alleviating the localized stress concentration in the mid-height region of the abutment.

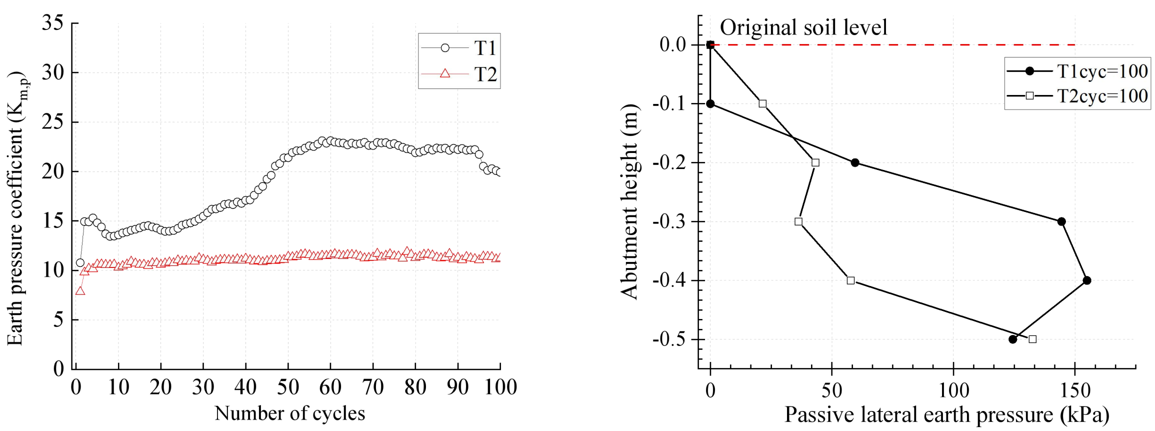

(a)Lateral earth pressure coefficient behind the abutment

(b) Distribution of lateral earth pressure along the abutment height

Fig. 3 Characteristics of lateral earth pressure behind the abutment

3.2 Backfill deformation

Figure 4 illustrates the evolution of the normalized vertical settlement (*h*/H) of the backfill over 100 loading cycles. For the T1 group, the settlement exhibited a pronounced and persistent cumulative increase. During the initial loading phase (the first 10 cycles), the steep gradient of the curve reflected rapid backfill subsidence. Although the settlement rate progressively diminished with increasing cycles, the cumulative magnitude continued to build up without any evidence of convergence by the 100th cycle, ultimately reaching a maximum value of approximately 29%. In contrast, the T2group demonstrated markedly improved deformation control. Not only was the initial rate of settlement accumulation substantially suppressed, but more significantly, the cumulative settlement progressively converged to a stable plateau after approximately 40 to 50 cycles, eventually attaining a steady state. By the 100th cycle, the final normalized vertical settlement (*h*/H) was effectively constrained to 14.5%. Compared to the T1 group, the maximum settlement magnitude was reduced by approximately 50%, demonstrating the superior efficacy of the reinforced configuration in mitigating cyclic subsidence.

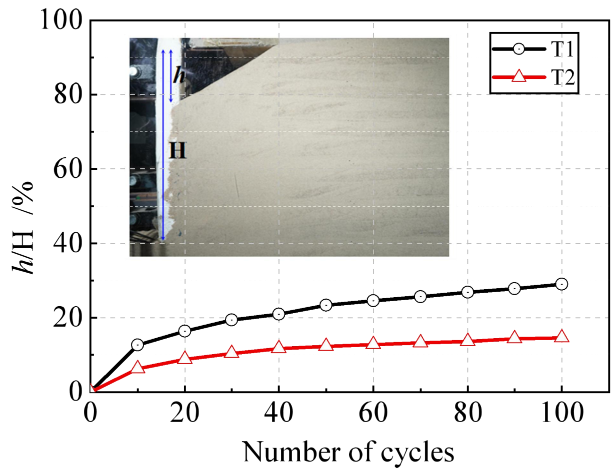

Fig. 4 Evolution of normalized backfill settlement with the number of cycles

4. Conclusions

Based on the 1g physical model tests investigating the soil-structure interaction within the integral abutment-approach slab-backfill system under the coupled effects of seasonal thermal and traffic loading, the following primary conclusions are drawn:

(1) The geogrid reinforcement effectively suppresses the cyclic ratcheting of passive earth pressures, significantly attenuates the peak lateral thrust, and facilitates a more homogeneous pressure distribution along the abutment. Compared to the unreinforced group (T1), the peak passive earth pressure coefficient ($K_{m,p}$) in the T2 reinforced configuration was reduced by approximately 50.2%.

(2) Geogrid reinforcement demonstrates superior efficacy in controlling backfill deformation, effectively restricting cumulative settlement. In the T2 group, the final normalized vertical settlement (*h*/H) converged to a stable plateau of 14.5%. Relative to the T1 group, the maximum settlement magnitude was substantially decreased by approximately 50%.

Acknowledgments

The authors gratefully acknowledge financial support from the National Natural Science Foundation of China (Grant Nos. 52578229 and 51878447) and the Tianjin Science and Technology Bureau Key Research and Development Program (Grant No. 23YFXTHZ00010).

References

[1] Hassan, M. S. K., Liyanapathirana, D. S., Fuentes, W., Leo, C. J., & Hu, P. (2024). A review of soil deformation and lateral pressure ratcheting phenomena in integral abutment bridges. Transportation Geotechnics, 49, 101388.

[2] Sigdel, L. D., Lu, M., Leo, C. J., Liyanapathirana, S., Hu, P., Doan, V., & Al-Qarawi, A. (2023). An experimental investigation into soil–structure interactions of integral bridge abutments due to cyclic translations. Canadian Geotechnical Journal, 61(2), 241-257.

[3] Liu, H., Han, J., Jawad, S., & Parsons, R. L. (2022). Effects of traffic loading on seasonal temperature change-induced problems for integral bridge approaches and mitigation with geosynthetic reinforcement. International Journal of Geomechanics, 22(6), 04022082.

[4] Cai, C. S., Shi, X. M., Voyiadjis, G. Z., & Zhang, Z. J. (2005). Structural performance of bridge approach slabs under given embankment settlement. Journal of Bridge Engineering, 10(4), 482-489.

[5] Zhao, Q., Wang, Y., Gui, K., Zhang, S., Huang, B., & Chen, Z. (2026). Progressive failure of backfill behind the integral bridge abutment due to seasonal temperature variation. Canadian Geotechnical Journal, (ja).

[6] Liu, H., Han, J., & Parsons, R. L. (2022). Geosynthetic reinforcement of backfill behind integral abutments to mitigate approach slab distresses. Engineering Structures, 269, 114772.